MINISTRY OF EDUCATION VIETNAM ACADEMY OF AND TRAINING SCIENCE AND TECHNOLOGY

GRADUATE UNIVERSITY SCIENCE AND TECHNOLOGY

CAO TRAN NGOC TUAN



DEVELOPMENT OF A TRAJECTORY CONTROL METHOD FOR ELECTRIC WHEELCHAIRS USING HIGHER-ORDER SLIDING MODE CONTROL

SUMMARY OF ELECTRICAL, ELECTRONICS AND TELECOMMUNICATION DOCTORAL THESIS

Major: Control Engineering and Automation

Code: 9 52 02 16

Ho Chi Minh city, 2025

This thesis is accomplished at: Graduate university Science and Technology - Vietnam Academy of Science and Technology

Supervisors:

- 1. Supervisors 1: Dr. Truong Nguyen Vu
- 2. Supervisors 2: Assoc. Prof Ha Quang Phuc

Referee 1: Prof. Dr. Nguyen Truong Thinh

Referee 2: Dr. Nguyen Nhu Son

Referee 3: Assoc. Prof. Dr. Le Hoang Thai

The dissertation is examined by Examination Board of Graduate University of Science and Technology, Vietnam Academy of Science and Technology at 9:00 a.m. on October 4, 2025.

The dissertation can be found at:

- 1. Graduate University of Science and Technology Library
- 2. National Library of Vietnam

LIST OF THE PUBLICATIONS RELATED TO THE DISSERTATION

- 1. TNT Cao, TB Pham, TN Nguyen, DL Vu, & NV Truong, 2024, Second-Order Terminal Sliding Mode Control for Trajectory Tracking of a Differential Drive Robot. Mathematics, 12(17), 2657
- 2. TNT Cao & Pham, Binh & Tran, Hieu & Gia, Long & Nguyen, No & Truong, Vu. (2024). Non-singular terminal sliding mode control for trajectory-tracking of a differential drive robot. E3S Web of Conferences. 496. 10.1051/e3sconf/202449602005.
- 3. Pham, Thanh-Binh & TNT Cao & Nguyen, Tan-No & Truong, Nguyen-Vu. (2025). Adaptive Full Order Sliding Mode Control for Electrical Motor Drive. E3S Web of Conferences. 626. 02001. 10.1051/e3sconf/202562602001.
- 4. Dang-Phuc Tran, TNT Cao, Duc-Hieu Tran, Tan-No Nguyen and Nguyen-Vu Truong. (2025). Electrical motor drive parameter estimation via higher order sliding mode control. E3S Web of Conferences. 626. 02002. 10.1051/e3sconf/202562602002

INRODUCTION

1. The necessary of thesis

The demand for electric wheelchairs has been steadily increasing due to various reasons. Specifically, according to statistics, as of 2025, approximately 12% of adults in the United States experience mobility limitations that cause serious difficulty in walking or climbing stairs, and around 5.5 to 6 million adults rely on wheelchairs for daily movement [1].

Among these users, about 10% report severe difficulties or an inability to operate powered wheelchairs for everyday activities, and 40% of powered wheelchair users encounter challenges in maneuvering—particularly in confined spaces or complex terrains [2]. These control difficulties often lead to serious accidents, 65–80% of which are related to tipping or falling incidents [3].

To address these issues, semi-autonomous and fully autonomous electric wheelchairs have emerged as promising solutions, enabling users—especially those with severe medical conditions or limited strength and dexterity—to control wheelchairs more effectively and safely.

In developing autonomous wheelchair systems, in addition to research on sensor integration for navigation or advanced human–computer interfaces (HCI) and brain–computer interfaces (BCI), one of the core and extensively studied problems is trajectory tracking control.

Trajectory control plays a crucial role because electric wheelchairs operate in complex environments with numerous uncertainties, including uncertainties in their own dynamic model (e.g., variations in mass or center of gravity) and external disturbances such as surface friction and slope variation.

Hence, a reliable trajectory control method is required to ensure stability, accuracy, and safety when navigating through complex terrains.

Given these challenges, Sliding Mode Control (SMC) has been regarded as a suitable approach compared to traditional control methods. However, despite its advantages, SMC suffers from a fundamental drawback known as "chattering", in which the control signal oscillates rapidly around the desired value. This phenomenon can degrade control accuracy and even damage electromechanical components.

Consequently, although numerous studies have applied SMC to trajectory control [4]-[18], considering uncertainties and disturbances, most have been limited to simulations or small-scale laboratory experiments due to the chattering effect.

Therefore, this dissertation focuses on developing a novel trajectory tracking control algorithm for electric wheelchairs based on high-order sliding mode control to overcome the chattering issue. Specifically, a second-order terminal sliding mode approach is proposed, offering advantages such as robustness against disturbances and uncertainties, high accuracy, and finite-time convergence. Moreover, its most significant benefit is the elimination of chattering, allowing the algorithm to be implemented directly on real electromechanical systems (i.e., electric wheelchairs).

2. Research Objective of the Thesis

Develop a trajectory control method for electric wheelchairs using highorder sliding mode control to address the "chattering" issue in sliding mode control, enabling direct practical application.

3. Main Research Content of the Thesis

Design a second-order Terminal Sliding Mode surface, including the ability to calculate the design parameters of the controller and the convergence time of state variables, applicable to practical electromechanical systems.

Design a trajectory controller for the Differential Drive Mobile Robot (DDMR) based on second-order Terminal Sliding Mode.

Apply the controller to a real DDMR system to demonstrate its robustness and effectiveness.

Thesis Content Structure

The thesis consists of 4 chapters:

Chapter 1: Presents an overview of previous studies on trajectory control of electric wheelchairs and differential drive mobile robots (DDMRs), as well as in-depth research on sliding mode control (SMC). Based on this review, the research direction and objectives of the dissertation are defined.

Chapter 2: Describes the theoretical background of sliding mode control and the modeling of DDMR systems. This chapter serves as the foundation for developing the new control theories presented in Chapters 3 and 4.

Chapter 3: Introduces the proposed second-order terminal sliding mode (2TSM) control theory, including the complete design of the sliding surface and the corresponding verification through simulations.

Chapter 4: Develops a trajectory tracking controller for the DDMR based on the 2TSM surface constructed in Chapter 3. The controller's performance is evaluated through comparisons with traditional control methods and validated by experimental results on a real system.

Conclusion

CHAPTER 1: OVERVIEW

1.1 Introduction

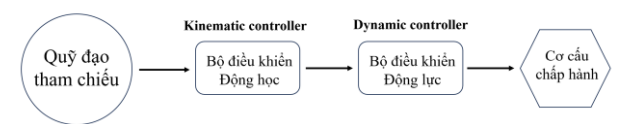


Figure 1.1 Simplified trajectory tracking controller structure

1.2 Related Studies

1.2.1 Studies on Traditional Trajectory Control of Electric Wheelchairs

The first studies on trajectory control of electric wheelchairs appeared in the late 1990s. In 1999, Caracciolo [27] and later Sun S. [28] in 2005 employed the linearization feedback control method for mobile robot trajectory control. Specifically, Sun S. applied the feedback linearization control approach based solely on the kinematic model. Similarly, in 2019, K. Maatoug [29] proposed a trajectory control method using a fuzzy controller, while in 2023, A. Amrane [30] introduced a control approach based on the PID controller. To improve control accuracy, some studies also considered the dynamic model. For instance, T. Fukao et al. [31] and Shojaei et al. [32] applied adaptive control to trajectory tracking. However, these studies rarely addressed system uncertainties or external disturbances and were mostly limited to simulation results.

1.2.2 Studies on Trajectory Control of Electric Wheelchairs Using SMC

In 2009, Solea [7] proposed a trajectory control approach using a conventional Sliding Mode Controller (SMC). Subsequently, many studies explored various SMC-based sliding surfaces. For example, B. B. Mevo [8] (2018) adopted an integral sliding surface, while J. Yang (1999) [11] and Lingrong (2011) [12] also proposed first-order SMC methods. Although these studies achieved promising results and accounted for uncertainties, they all suffered from the chattering phenomenon.

1.2.3 Studies on Chattering Suppression in SMC

In 1977, Utkin [37] introduced the boundary layer method, a simple and widely used approach to reduce chattering. The concept of higher-order sliding surfaces was later proposed in 1998 by G. Bartolini [42] and Levant

[43]-[44]. In 2014, Y. Feng [49] proposed a full-order Terminal Sliding Mode (TSM), and in 2021, Xinghuo Yu and Yong Feng [50] provided a comprehensive review of various SMC techniques, particularly in Terminal Sliding Mode Control (TSMC) and its higher-order forms aimed at mitigating chattering.

Although higher-order TSMC methods effectively suppress chattering while maintaining robustness, they often lack analytical formulations for controller parameters and convergence time, limiting their practical applications. Therefore, this dissertation investigates a second-order Terminal Sliding Mode (2TSM) surface to address these two issues and optimize chattering suppression for the DDMR system.

1.3 Conclusion

1.3.1 Summary of Current Research Status

1.3.2 Research Issues in the Dissertation

Investigate the design of a second-order Terminal Sliding Mode (2TSM) surface with the capability to calculate controller parameters and convergence time.

Study the design of a trajectory controller for the Differential Drive Mobile Robot (DDMR) based on 2TSM, accounting for model uncertainties.

Conduct experiments on a real DDMR system.

1.3.3 Scope of the Research

The dissertation focuses on the development of a new control algorithm. Therefore, in conducting experiments, the author employs a mobile robot model under scenarios with uncertainties, which facilitates the tuning and modification of the algorithm, rather than performing experiments on a fully developed electric wheelchair.

CHAPTER 2: SLIDING MODE CONTROL THEORY AND SYSTEM MODELING

2.1 Sliding Mode Control Theory

2.1.1 Historical Background

2.1.2 Concepts of Stability

2.1.2.1 Asymptotic Stability

$$x(t) \to 0$$
 khi $t \to \infty$ (2.1)

***** When uncertainties are present:

If Δf represents unknown disturbance factors, instead of converging to "0", the system's state will converge to:

$$x(t) \to \frac{\Delta f}{\gamma} \quad khi \quad t \to \infty$$
 (2.2)

2.1.2.2 Finite-Time Stability

$$x(t) \to 0$$
 tại $t = \frac{x(0)^{1-p/q}}{\gamma(1-p/q)}$ (2.3)

Where p, q are odd number and p/q < 1

***** When uncertainties are present:

N If Δf represents unknown disturbance factors:

$$\to x(t) = \left(\frac{\Delta f}{\gamma}\right)^{\frac{q}{p}} \tag{2.4}$$

This means that using a control signal to bring the system to an equilibrium state in finite time will result in a smaller steady-state error compared to asymptotic stability.

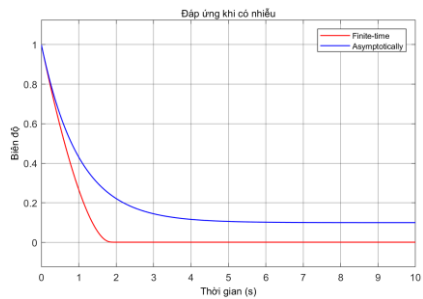


Figure 2.1 System response under uncertainties

$$(\gamma = 1, \Delta f = 0.1, p/q = 1/3)$$

Conclusion: From the above, it can be observed that the control of a system with a "finite-time" response has several advantages over an "asymptotic" response, including:

- Faster convergence speed.
- Higher control accuracy.

Based on these concepts, the thesis will analyze the advantages and disadvantages of linear and nonlinear sliding surfaces in the following section.

2.1.3 Idea of Sliding Mode Control

2.1.3.1 Linear Sliding Mode (LSM)

Consider the follow system:

$$\begin{cases} \dot{x}_1 = x_2 \\ \dot{x}_2 = f(x) + u + \rho(x, t) \end{cases}$$
 (2.5)

Firstly, the sliding manifold was designed:

$$s = x_2 + \gamma x_1, \gamma > 0 \tag{2.6}$$

when s=0, the system state x_1, x_2 will converge asymptotically to "0" in natural response: $\dot{x}_1 = -\gamma x_1$

The control law was designed as follow:

$$u = u_{eq} + u_n \tag{2.7}$$

where:

$$u_{eq} = -f(x) - \gamma x_2 \tag{2.8}$$

$$u_n = -k sign(s)$$

With the above control law, $s \rightarrow 0$ in finite time:

$$t_r = \frac{\sqrt{2}}{\eta} V^{\frac{1}{2}}(0) \tag{2.9}$$

2.1.3.2 Terminal Sliding Mode Control (TSM)

First, the nonlinear manifold was designed as:

$$s = x_2 + \gamma x_1^{p/q}, \gamma > 0 (2.10)$$

With $0 < \frac{p}{q} < 1$ and p, q are odd interger. When s = 0, the state variables x_1, x_2 will converge to "0" according to: $\dot{x}_1 = -\gamma x_1^{p/q}$

The control law was designed as follow:

$$u = u_{eq} + u_n$$

$$u_{eq} = -f(x) - \gamma p / q x_1^{p/q-1} \dot{x}_1$$

$$u_n = -k sign(s)$$
(2.11)

Remark: in the control signal: $ueq = -f(x) - \gamma \frac{p}{q} x_1^{\frac{p}{q}-1} \dot{x}_1$ has the possibility of encountering a singularity poin $x_1 = 0$, $\dot{x}_1 \neq 0$. Figure 2.2 (t = 0.37s).

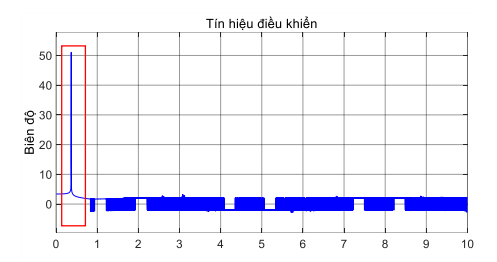


Figure 2.2 the control signal with singularity point

2.1.3.3 Nonsingular Terminal Sliding Mode Control (NTSM)

$$s = x_1 + \frac{1}{\gamma} x_2^{q/p} \tag{2.12}$$

When s = 0, the response of NTSM (2.12) equivalent to (2.10) The control law $u = u_{eq} + u_n$ was designed as follow:

$$\begin{cases} u_{eq} = -f(x) - \gamma \frac{p}{q} x_2^{2-q/p} \\ u_n = -k sign(s) \end{cases}$$
 (2.13)

Applied the control law (2.13), it gets:

$$\dot{V} = s \frac{1}{\gamma} \frac{q}{p} x_2^{\frac{q}{p} - 1} (-k sign(s) + \rho(t))$$

Conclusion: Control signal $u_{eq} = -f(x) - \gamma \frac{p}{q} x_2^{2-q/p}$ was eliminated the singularity point at $x_2 = 0, x_1 \neq 0$.

The inherent disadvantage of Sliding Mode Control (SMC) is the phenomenon of "chattering." Research efforts aimed at eliminating this "chattering" phenomenon will be presented in the following section.

2.1.4 Chattering problem

2.2 System modeling

2.2.1 Introduction

2.2.2 Kinematic model

❖ Forward kinematic:

$$\begin{cases} v = \frac{v_r + v_l}{2} = \frac{R(\dot{\varphi}_r + \dot{\varphi}_l)}{2} \\ \omega = \frac{v_r - v_l}{2L} = \frac{R(\dot{\varphi}_r - \dot{\varphi}_l)}{2L} \end{cases}$$
(2.14)

❖ Inverse kinematic:

$$\begin{cases} v_r = v + \omega L \\ v_l = v - \omega L \end{cases} \tag{2.15}$$

2.2.3 Dynamic model

$$\left(m + \frac{2}{R^2} I_w\right) \dot{v} - m_c d\omega^2 = \frac{1}{R} (\tau_r + \tau_l)$$

$$\left(I + \frac{2L^2}{R^2} I_w\right) \dot{\omega} + m_c d\omega v = \frac{L}{R} (\tau_r - \tau_l)$$
(2.16)

2.2.4 Uncertainties in the model

- Uncertainty about the mass: limited to 50 100 (kg)
- Change in the center of mass: limited to $\Delta d = 15$ (cm)

$$M_0 \begin{bmatrix} \dot{v} \\ \dot{\omega} \end{bmatrix} = V_0 + C \begin{bmatrix} \tau_r \\ \tau_l \end{bmatrix} \underbrace{+\Delta V - \Delta M \begin{bmatrix} \dot{v} \\ \dot{\omega} \end{bmatrix} + d(t)}_{\rho(t)}$$
(2.17)

Where M_0 , V_0 are the known initial values, ΔM and ΔV are the changing quantities, d(t) is other uncertainties, $\rho(t)$ is the total uncertainties values.

2.3 Conclusion

CHAPTER 3. DESIGN OF HIGH-ORDER SLIDING SURFACES

3.1 Methods for Eliminating "Chattering" in Sliding Mode Control

3.1.1 Method using boundary layer

- 3.1.1.1 Method using the saturation function
- 3.1.1.2 Method using the sigmoid function

3.1.2 Higher-order sliding mode method

3.1.2.1 Higher-order LSM sliding surface

The sliding manifold is proposed:

$$s = \ddot{x} + \alpha \dot{x} + \beta x \tag{3.1}$$

Control law $u = u_{eq} + u_n$ is designed as follow:

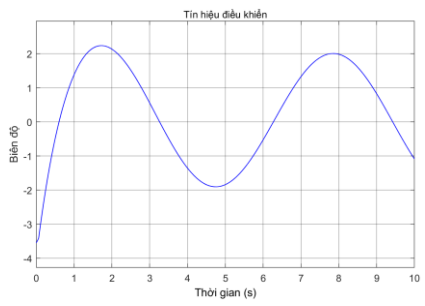
$$\begin{cases}
 u_{eq} = -f(x) - \alpha \dot{x}_1 - \beta x_1 \\
 \dot{u}_n = -k sign(s)
\end{cases}$$
(3.2)

Ex: We design the sliding surface and control signal as follows:

$$s = \ddot{x}_1 + 2\dot{x}_1 + x_1$$
$$u = 0.1x_2 - 2\dot{x}_1 - x_1 - 5\int_0^t sign(s)dt$$

The simulation results are shown in Figure 2.3.

It can be observed that although the control signal is smooth and chattering is eliminated, the drawback of the linear sliding surface remains: the state variable does not reach zero but only converges asymptotically.



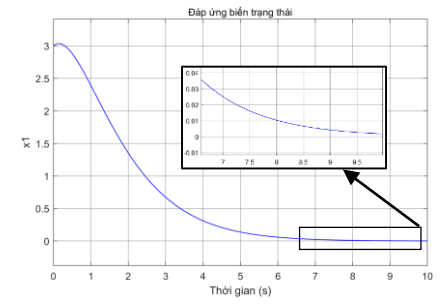


Figure 3.1 Control signal

Figure 3.2 State response

3.1.2.2 Full order Terminal Sliding Mode (FOTSM)

According to [46], the sliding surface is chosen as follows:

$$s = \dot{x}_n + c_n sgn(x_n)|x_n|^{\alpha_n} + \dots + c_1 sgn(x_1)|x_1|^{\alpha_1}$$
 (3.3)

where c_i , α_i (i=1,2,...n) are constant. c_i is chosen such as $p^n + c_n p^{n-1} + \cdots + c_2 p + c_1$ is Hurwitz, and α_i is chosen as follows

$$\begin{cases} \alpha_1 = \alpha, & n = 1 \\ \alpha_{i-1} = \frac{\alpha_i \alpha_{i+1}}{2\alpha_{i+1} - \alpha_i}, & i = 1, 2, \dots, n \ \forall n \ge 2 \end{cases}$$
 (3.4)

Where: $\alpha_{n+1} = 1$, $\alpha_n = \alpha$, $\alpha \in (1 - \varepsilon, 1)$, $\varepsilon \in (0,1)$.

Applying it to system (2.5), we obtain the sliding surface:

$$s = \ddot{x}_1 + c_2 sign(\dot{x}_1) |\dot{x}_1|^{\alpha_2} + c_1 sign(x_1) |x_1|^{\alpha_1}$$
(3.5)

Control law $u = u_{eq} + u_n$ is designed as follow:

$$u_{eq} = -f(x) - c_2 sign(\dot{x}_1)|\dot{x}_1|^{\alpha_2} - c_1 sign(x_1)|x_1|^{\alpha_1}$$

$$\dot{u}_n + \lambda u_n = v; v = -(k_d + k_T + \eta) sign(s)$$
(3.6)

Example: Consider the same system as above. We design the sliding surface and control signal as follows:

$$\begin{split} s &= \ddot{x}_1 + 2sign(\dot{x}_1)|\dot{x}_1|^{9/16} + sign(x_1)|x_1|^{9/23} \\ &\to u = u_{eq} + e^{-0.1t} \int_0^t e^{-0.1t} v dt \end{split}$$

Where e is the base of the natural logarithm. $(\ln(e) = 1)$.

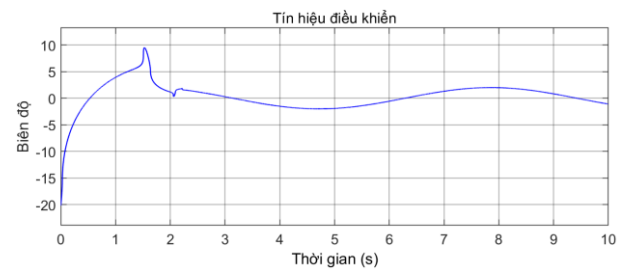


Figure 3.3 Control signal FOTSM

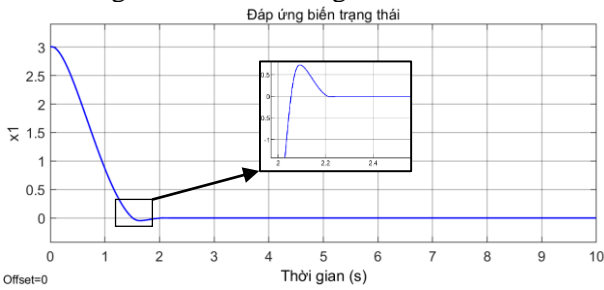


Figure 3.4 State response FOTSM

It can be observed that the control signal has almost completely eliminated chattering (Figure 3.3) and the state variable has converged to zero (Figure 3.4). However, this method currently has two major issues that prevent its practical application: it cannot be computed and it cannot be measured.

3.1.3 Comparison and Selection of Methods

The Full-Order Terminal Sliding Mode (FOTSM) method is considered the optimal approach for suppressing chattering in sliding mode control, provided that its current limitations can be effectively addressed.

3.2 Second-Order Terminal Sliding Surface

3.2.1 Design of Sliding Surface

The second order TSM manifold is chosen as follow:

$$s = \ddot{x} + \gamma_1 \dot{x}^\alpha + \gamma_2 x^\beta \tag{3.7}$$

Wherein, the following conditions are satisfied:

$$0 < \alpha = \frac{q}{p} < 1, \beta = \frac{\alpha}{2-\alpha} = \frac{q}{2p-q}, p > q \text{ are odd intergers};$$

$$0 < \gamma_1; \ \gamma_2 = \gamma_1^{\beta+1} \frac{\alpha^{\beta}}{(\beta+1)^{\beta}} \left(1 - \frac{\alpha}{2}\right) > 0;$$

$$x(0) = x_0, \dot{x}(0) = -\gamma_1^{\beta/\alpha} \left(\frac{\alpha}{\beta+1}\right)^{\beta/\alpha} x_0^{1/(2-\alpha)}.$$

$$(3.8)$$

Theorem 1: when the manifold (3.7) converge to 0 (s = 0) and the conditions (3.8) is satisfied, the state variable x(t) and its derivative $\dot{x}(t)$ converge to 0 in finite time, which is calculated as follow:

$$t_{convergence} = \frac{\alpha}{\alpha - \beta} \left(\frac{\gamma_1 \alpha}{\beta + 1} \right)^{-\beta/\alpha} \chi_0^{(\alpha - \beta)/\alpha}$$
(3.9)

Prove:

Take $y = \dot{x} \rightarrow \ddot{x} = y \frac{dy}{dx}$, s = 0, (3.7) become:

$$F(y, \dot{y}) = y \frac{dy}{dx} + \gamma_1 y^{\alpha} = -\gamma_2 x^{\beta}$$
(3.10)

natural response of (3.10) is:

$$F(y, \dot{y}) = y \frac{dy}{dx} + \gamma_1 y^{\alpha} = 0$$
(3.11)

Where y = 0 is particular solution of (3.11), in the case $y \neq 0$, (3.11) is rewritten as: $y^{1-\alpha}dy = -\gamma_1 dx$.

Integrating both sides, we obtain:

$$\frac{1}{2-\alpha}y^{2-\alpha} = -\gamma_1 x + C$$

$$y = (Mx + N)^{1/(2-\alpha)}$$
(3.12)

With the presence of the signal $u = -\gamma_2 x^{\beta}$, the general solution has the form:

$$y = (Mx + f(x))^{1/(2-\alpha)}$$
 (3.13)

Where N = f(x) is the function of x. Substituting (4.7) into (4.4), we obtain:

$$\left(\gamma_1 + \frac{M + \frac{df}{dx}}{2 - \alpha}\right) \left(Mx + f(x)\right)^{\beta} = -\gamma_2 x^{\beta}$$
(3.14)

where

- Mx + f(x) has the form Mx + f(x) = Kx; derive f(x) = (K - M)x- $\frac{df}{dx} = (K - M)$

Equating both sides, we obtain:

$$\left(\gamma_1 + \frac{K}{2 - \alpha}\right) K^{\beta} = -\gamma_2 \tag{3.15}$$

From (3.15), it easy to see: if $\gamma_2 > 0$, K < 0, then:

The minimum of
$$g(K) = \left(\gamma_1 + \frac{K}{2-\alpha}\right)K^{\beta} + \gamma_2$$
 exits at $K^* = -\gamma_1 \frac{\beta(2-\alpha)}{\beta+1} = -\gamma_1 \frac{\alpha}{\beta+1}$

-
$$g\left(K^* = -\gamma_1 \frac{\alpha}{\beta + 1}\right) = 0$$
 and K^* is the unique solution of (3.15)

The result is:

$$y = (K^*x)^{1/(2-\alpha)} = \underbrace{-\left[\gamma_1 \frac{\alpha}{\beta+1}\right]^{1/(2-\alpha)}}_{A} x^{1/(2-\alpha)}$$

Then, the general solution is

$$y = \dot{x} = Ax^{1/(2-\alpha)} \tag{3.16}$$

Remark : Picard – Lindelöf theorem assert that (3.16) is the unique solution of the equation. $F(y, \dot{y}) = y \frac{dy}{dx} + \gamma_1 y^{\alpha} = -\gamma_2 x^{\beta}$ according to the given initial conditions.

Hoàn tất chứng minh.

3.2.2 Simulation of sliding surface convergence time:

With $\gamma_1, \gamma_2, \alpha, \beta$ are chosen in theorem 3, the desire convergence time is t = 2s, the sliding manifold is designed as follow:

$$s = \ddot{x} + 9.92\dot{x}^{3/5} + 12.8x^{3/7} = 0 \tag{3.17}$$

With the initial variable $x_0 = 5$, the systems response as in Figure 4.5:

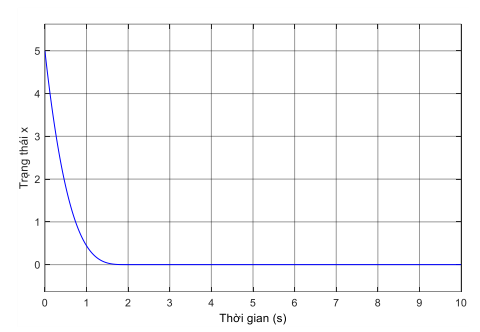


Figure 3.5 Simulation results of the natural convergence of the 2TSM surface.

3.3 Conclusion

In this chapter, the dissertation has presented a complete theoretical development of the Second-Order Terminal Sliding Surface (2TSM). The

proposed approach successfully addresses two long-standing issues in conventional Terminal Sliding Mode Control: the ability to analytically determine the sliding surface parameters, and the capability to estimate the convergence time of the system's state variables.

CHAPTER 4. DESIGN OF TRAJECTORY TRACKING CONTROLLER BASED ON 2TSM SLIDING SURFACE

4.1 Trajectory control method

Based on the pre-designed trajectory, the reference DDMR will move ahead, and the actual DDMR will follow. The control diagram is shown in Figure 4.1.

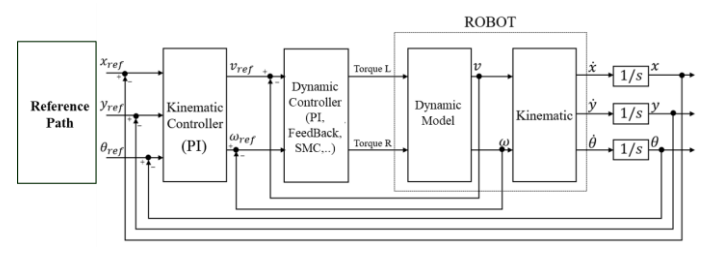


Figure 4.1 Trajectory control diagram

Kinematic Controller:

The tracking error p_e is the different between real and refference position, denoted as $p = [x \ y \ \theta]^T$ and the refference position, denoted as $p_{ref} = [x_{ref} \ y_{ref} \ \theta_{ref}]^T$, it obtain:

$$p_e = \begin{bmatrix} x_e \\ y_e \\ \theta_e \end{bmatrix} = p_{ref} - p = \begin{bmatrix} x_{ref} - x \\ y_{ref} - y \\ \theta_{ref} - \theta \end{bmatrix}$$
(4.1)

The outermost kinematic controller uses a simple P-type controller, designed as follows:

$$\omega_{ref} = K_w.\theta_e, v_{ref} = K_v.d_e \tag{4.2}$$

where ω_{ref} , v_{ref} are the refference velocities; K_w , K_v are the gain controller; $d_e=(x_e^2+y_e^2)^{1/2}$ và $\theta_e=tan^{-1}(y_e,x_e)$.

Dynamic Controller:

After the signals ω_{ref} , v_{ref} are sent to the dynamic controller, it calculates and generates the control signals—torques τ_{right} , τ_{left} - to each wheel (Figure 4.2).

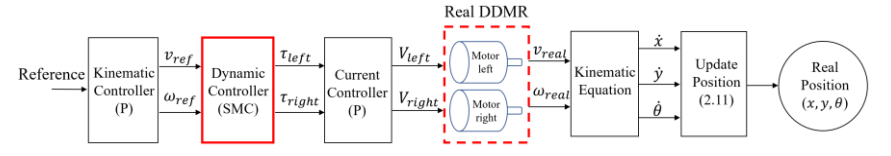


Figure 4.2 Trajectory control flowchart in simulation

4.2 Using Linear Sliding Mode (LSM)

4.2.1 Controller design (LSM sliding surface)

$$M\ddot{q} = V(\dot{q}) + Cu(t) + \rho(t) \tag{4.3}$$

The error is defined as:

$$\dot{e}(t) = \dot{q} - \dot{q}_r = [v_e, \, \omega_e]^T = \left[v - v_{ref}, \, \omega - \omega_{ref}\right]^T \tag{4.4}$$

Sliding manifold: $s = \dot{e} + \gamma e$

The control law is: $u = u_{eq} + u_n$

$$\begin{cases} u_{eq} = C^{-1}M(-M^{-1}V(\dot{q}) + \ddot{q}_r - \gamma \dot{e}) \\ u_n = -C^{-1}Msign(s)(k+\eta) \end{cases}$$
(4.5)

4.2.2 Simulation

4.2.2.1 LSM without "boundary layer"

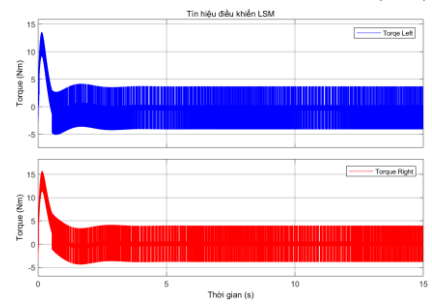


Figure 4.3 Trajectory 1 control signal (without boundary layer)

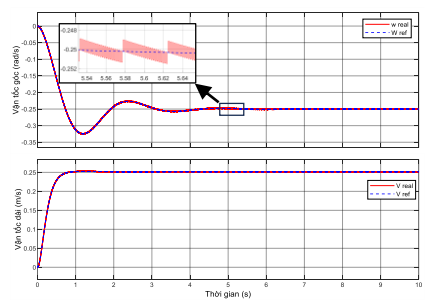


Figure 4.4 Velocities response (trajectory 1 - without boundary layer)

4.2.2.2 LSM with boundary layer

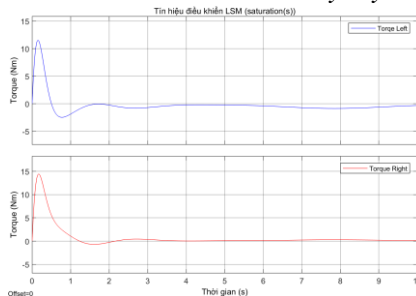


Figure 4.5 Trajectory 1 control signal (with boundary layer)

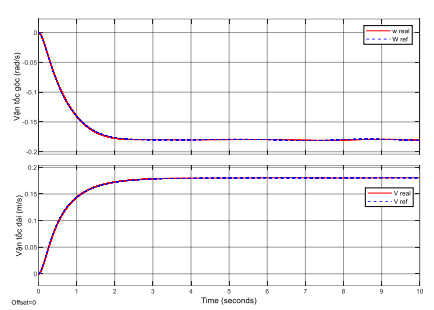


Figure 4.6 Velocities response (trajectory 1 - with boundary layer)

4.3 Using nonliner sliding surface (NTSM)

4.3.1 Controller design (NTSM sliding surface)

$$s = e + \frac{1}{\gamma} \dot{e}^{q/p} \tag{4.6}$$

Theorem 2: Control law is: $u = u_{eq} + u_n$

Where:

$$u_{eq} = C^{-1} M \left(-M^{-1} V(\dot{q}) + \ddot{q}_r - \gamma \frac{p}{q} \dot{e}^{2-q/p} \right) \eqno(4.7)$$

$$u_n = -C^{-1}Msign(s)(k+\eta)$$
(4.8)

And satisfied the condition: $k = Max\{||M^{-1}\rho(t)||\}$, $\eta > 0$

4.3.2 Simulation

4.3.2.1 NTSM without "boundary layer"

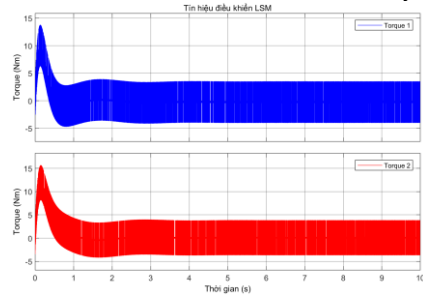


Figure 4.7 Trajectory 1 control signal (NTSM without boundary layer)

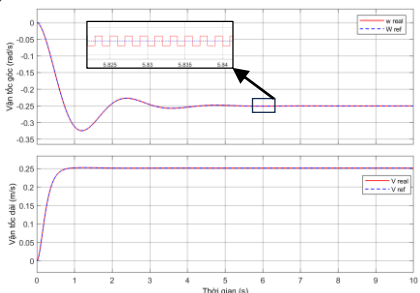


Figure 4.8 Velocities response (trajectory 1 – NTSM without boundary layer)

4.3.2.2 Mô phỏng NTSM với boundary layer

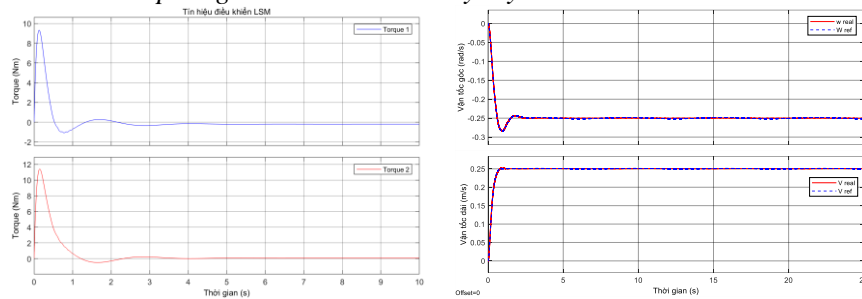


Figure 4.9 Trajectory 1 control signal (NTSM with boundary layer)

Figure 4.10 Velocities response (trajectory 1 – NTSM with boundary layer)

4.4 Using Second-Order TSM Sliding Surface

4.4.1 Controller Design

Theorem 3: The velocity error of the system will converge to zero when the control signal is designed as follows: $u = u_{eq} + u_n$

$$u_{eq} = C^{-1}M(-M^{-1}V + \ddot{q}_r - \gamma_1 \dot{e}^{\alpha} - \gamma_2 e^{\beta})$$

$$\dot{u}_n = C^{-1}M(sign(s)(k+\eta))$$
(4.9)

Where $k = Max\{||M^{-1}\dot{\rho}(t)||\} \text{ và } \eta > 0$

Prove:

By substituting the system state errors into the 2TSM sliding surface, we obtain:

$$s = M^{-1} \big(V(\dot{q}) + C\tau(t) + \rho(t) \big) - \ddot{q}_r + \gamma_1 \dot{e}^{\alpha} + \gamma_2 e^{\beta}$$

Substituting the control signal (4.12) into the above expression:

$$s = M^{-1}Cu_n + M^{-1}\rho(t)$$

Consider Lyapunov function: $V = 0.5s^T s$, it gets:

$$\dot{V} = s^T \dot{s} = s^T \left(-sign(s)k - sign(s)\mu + M^{-1}\dot{\rho}(t) \right) \tag{4.10}$$

It follow that:

$$\begin{split} \dot{V} & \leq -k\|s\| - \eta\|s\| + M^{-1}\dot{\rho}(t) \leq -\eta\|s\| = -\eta\sqrt{2}V^{1/2} < 0 \\ s & \to 0 \text{ in finite time } t_r \leq \frac{\sqrt{2}V^{1/2}(0)}{n} \,. \end{split}$$

This completes the proof.

4.4.2 Simulation

The sliding surface and control signal are designed as follows:

$$s = \ddot{e} + 4\dot{e}^{3/5} + 3.49e^{3/7}$$

$$u_{eq} = C^{-1}M\left(-M^{-1}V + \ddot{q}_r - 4\dot{e}^{\frac{3}{5}} - 3.49e^{\frac{3}{7}}\right)$$

$$\dot{u}_n = C^{-1}M\left(sign(s)([2;1]^T + 0.2)\right)$$

The simulation results from Figure 4.11 to Figure 4.14.

• **Trajectory 1:** circle with a radius of 1 meter.

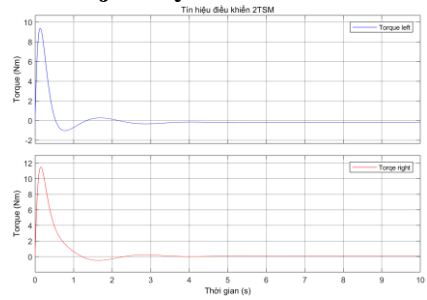


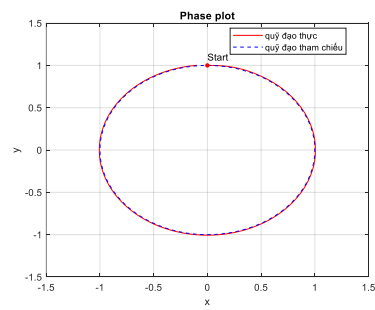
Figure 4.11 Trajectory 1 – control signal (2TSM)

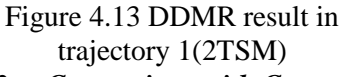
Figure 4.12 Trajectory 1 – velocities response (2TSM)

It can be seen that the 2TSM controller has eliminated the chattering phenomenon in the control signal (Figure 4.11) while maintaining high accuracy.

• **Trajectory 2:** A path consisting of straight segments combined with 90° turns.

For trajectory 2, the 2TSM controller still demonstrates robustness and high accuracy (Figure 4.14).





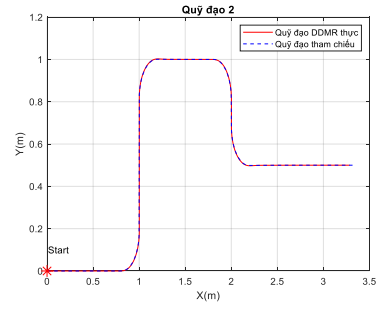


Figure 4.14 DDMR result in trajectory 2 (2TSM)

4.4.3 Comparison with Conventional Sliding Mode Controllers

Table 4.1 Longitudinal Velocity Error Responses of Different Methods

No	Response Parameters	Unit	NTSM boundary	NTSM	2TSM
1	Steady state errors	m/s	2e-3	-1.2e-4	-2.7e-8
2	(IAE)	m/s	5e-2	2.09e-3	1.6e-5

Bảng 4.2 Đáp ứng sai số vận tốc góc giữa các phương pháp

No	Response Parameters	Unit	NTSM boundary	NTSM	2TSM
1	Steady state errors	m/s	-4e-2	1.07e-3	9.6e-7
2	(IAE)	m/s	3.6e-2	8e-3	1.37e-5

The results clearly indicate that, in terms of both the steady-state error and the IAE index, the proposed 2TSM controller outperforms the conventional control methods. These findings confirm the superiority and practical effectiveness of the proposed controller design.

4.5 Experiment

4.5.1 DC motor control

4.5.1.1 Simulation

From the simulation, it can be seen that all four control methods exhibit comparable responses, each bringing the system to a convergent state in approximately 1 second. Among them, the 2TSM method (Figure 4.10) demonstrates superior performance by ensuring high accuracy, driving the error to zero, and eliminating chattering.

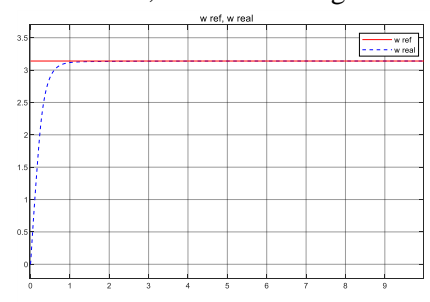


Figure 4.15 Motor velocity response (PID)

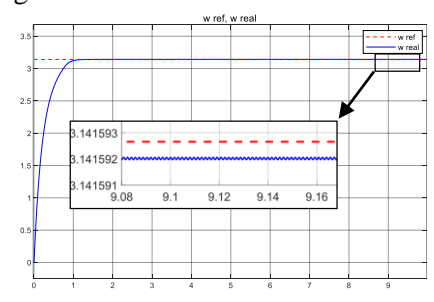


Figure 4.16 Motor velocity response (LSM)

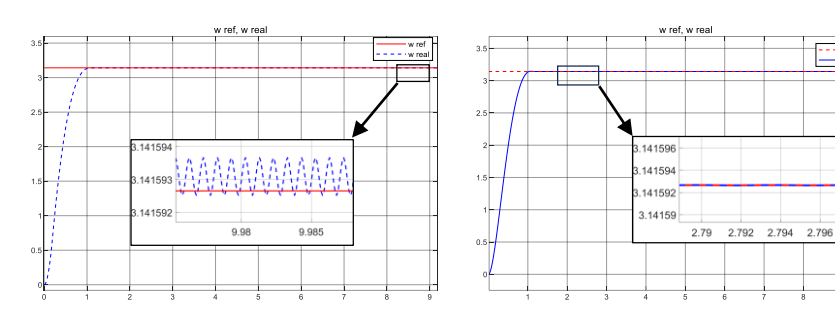
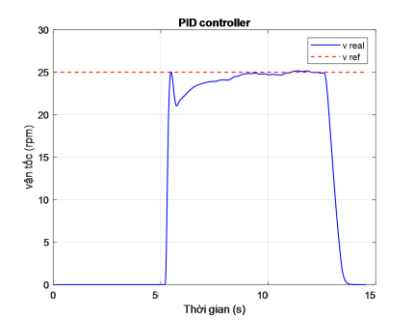


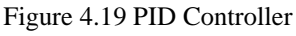
Figure 4.17 Motor velocity response (NTSM)

Figure 4.18 Motor velocity response (2TSM)

4.5.1.2 Experiment

Scenario 1: Constant reference speed without controller tuning





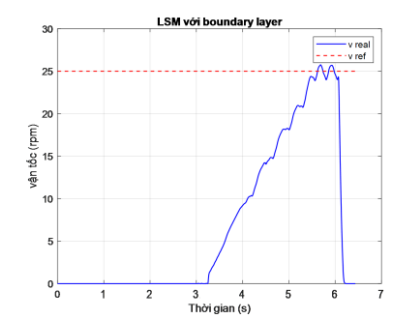


Figure 4.20 LSM ($\varepsilon = 0.01$)

Through the above experiments and simulations, the thesis has demonstrated the outstanding advantages of 2TSM in maintaining the characteristic robustness of SMC, the high accuracy of TSM, and the ability to eliminate chattering for direct application in practical control systems, forming the basis for applying it to trajectory control experiments.

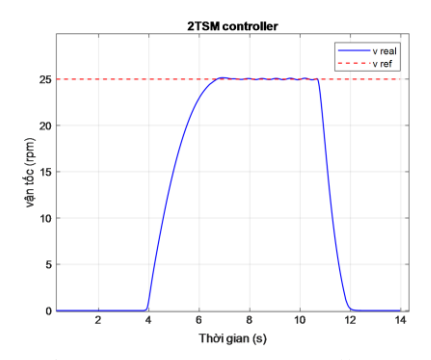
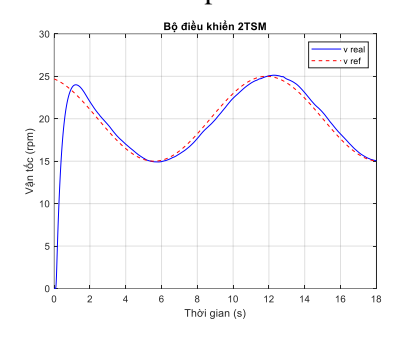


Figure 4.21 2TSM controller **Scenario 2:** Experiment with varying reference speed



30

Bộ điều khiến 2TSM

25

20

20

30

5

10

10

5

Thời cian (s)

Figure 4.22 Response of the PID controller with varying reference speed

Figure 4.23 Response of the 2TSM controller with varying reference speed

4.5.2 Trajectory Control

Dimension (DxRxC)	20x20x20 cm		
Wheel radius	6 cm		
Wheelbase distance	23.5 cm		
Power (DC)	12VDC 6000mah		

Scenario 1: A 3.5 kg load is placed at the center of gravity of the DDMR.

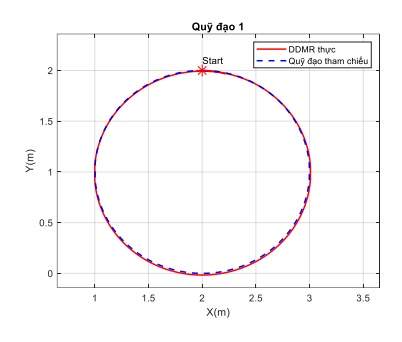
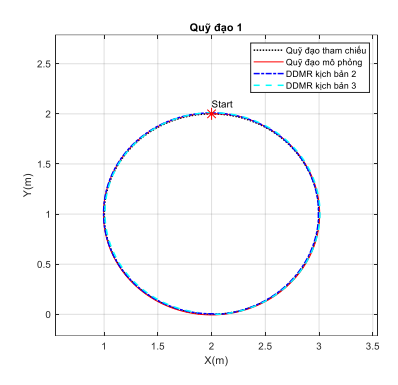


Figure 4.24 DDMR follow trajectory 1

Figure 4.25 DDMR follow trajectory 2

Scenarios 2 and 3: A 3.5 kg load is placed 5 cm to the left of the DDMR's center of gravity.



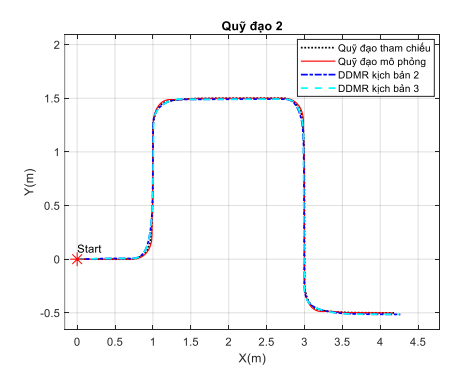


Figure 4.26 DDMR follow trajectory 1 (2&3)

Figure 4.27 DDMR follow trajectory 2 (2&3)

4.6 Conclusion:

The trajectory control method based on 2TSM, as designed in Chapter 4, has fully met the requirements set forth in the thesis, as demonstrated through both simulations and experiments.

CONCLUSION

Main Research Contents of the Thesis

The dissertation focuses on addressing the main drawback of Sliding Mode Control (SMC) — the chattering phenomenon — while preserving its key advantages of robustness against uncertainties and high precision.

In Chapter 2, the dissertation presents the theoretical foundations of SMC and the modeling of the DDMR system, including the uncertainties that need to be managed. Building on this theoretical basis, Chapter 3 analyzes the advantages and disadvantages of existing chattering reduction methods based on higher-order sliding surfaces and develops the Second-Order Terminal Sliding Mode (2TSM) surface. Using this 2TSM surface, Chapter 4 introduces the trajectory controller design and presents experimental results to demonstrate the controller's effectiveness.

New Scientific Contributions of the Thesis

The thesis has two main contributions:

- ➤ Designing a complete second-order Terminal Sliding Mode (TSM) sliding surface with the capabilities to:
 - Eliminates chattering in the control signal while maintaining SMC robustness,
 - Ensures system states converge to equilibrium in finite time,
 - Allows analytical computation of controller parameters,
 - Enables estimation of state response time,
 - Facilitates easy controller tuning.
- Designing a trajectory (dynamic) controller for the DDMR system, taking into account model uncertainties and unknown disturbances.

Research direction of the dissertation:

Develop a complete autonomous electric wheelchair control solution capable of navigating within designated indoor/outdoor environments.

Further extend the proposed sliding mode theory to torque control systems in other electromechanical systems such as robotic arms, drones, and similar applications.